Enhanced broadband near-IR luminescence and gain spectra of bismuth/erbium co-doped fiber by 830 and 980 nm dual pumping

Qiancheng Zhao, Yanhua Luo, Wenyu Wang, John Canning, and Gang-Ding Peng

Citation: AIP Advances **7**, 045012 (2017); doi: 10.1063/1.4981903
View online: http://dx.doi.org/10.1063/1.4981903
View Table of Contents: http://aip.scitation.org/toc/adv/7/4
Published by the American Institute of Physics

Enhanced broadband near-IR luminescence and gain spectra of bismuth/erbium co-doped fiber by 830 and 980 nm dual pumping

Qiancheng Zhao,[1,a] Yanhua Luo,[1] Wenyu Wang,[1] John Canning,[2] and Gang-Ding Peng[1]
[1]*Photonics and Optical Communication, School of Electrical Engineering and Telecommunications, University of New South Wales, Kensington, NSW 2052, Australia*
[2]*Interdisciplinary Photonics Laboratories, School of Chemistry, University of Sydney, NSW 2006, Australia*

(Received 10 January 2017; accepted 10 April 2017; published online 18 April 2017)

A dual 830 and 980 nm pumping scheme is proposed aiming at broadening and flattening the spectral performance of bismuth/erbium codoped multicomponent fiber (BEDF). The spectral properties of distinct Bi active centers (BACs) associated with germanium (BAC-Ge), aluminium (BAC-Al), phosphorus (BAC-P) and silicon (BAC-Si) are characterized under single pumping of 830 and 980 nm, respectively. Based on the emission slope efficiencies of BAC-Al (~1100 nm) and BAC-Si (~1430 nm) under single pumping of 830 and 980 nm, the dual pumping scheme with the optimal pump power ratio of 25 (980 nm VS 830 nm) is determined to achieve flat, ultrabroadband luminescence spectra covering the wavelength range 950-1600 nm. The dual pumping scheme is further demonstrated on the on-off gain performance of BEDF. It is found under the pump power ratio of ~8 (980 VS 830 nm), The gain spectrum has been flattened and broadened over 300 nm (1300-1600 nm) with an average gain coefficient of ~1.5 dBm^{-1}. The spectral coverage is approximately 1.5 and 3 times wider compared to single pumping of 830 and 980 nm pumping, respectively. The energy level diagrams of 830 and 980 nm are also constructed separately in view of the optical characteristic, which further clarifies the advantage for dual pumping. The proposed dual 830 and 980 nm pumping scheme with the multicomponent BEDF shows great potential in various broadband optical applications such as uniform ASE source, broadband amplifier and tuneable laser in NIR band. [http://dx.doi.org/10.1063/1.4981903]

Since the first discovery of near infrared (NIR) luminescence in bismuth (Bi)-doped silicate glass in 1999,[1] great attention has been paid to Bi-doped devices aiming at exploiting spectral gaps (1.1-1.5 μm) for rare earth doped media.[2–5] In addition, erbium-doped fiber amplifiers (EDFA) with high gain (several tens of dB) coefficient covering the range 1520-1620 nm have been commercially available.[6,7] Hence, Bi/Er codoped photonic devices are introduced to achieve ultrabroadband amplification covering the whole O-, E-, S-, C- and L-bands. Peng *et al.* firstly reported the spectral properties of Bi/Er codoped germanate glass under 808 nm pumping in 2010. However, no gain was reported due to excessive concentration of Bi ions.[8] The first Bi/Er codoped fiber (BEDF) was reported by Qiu *et al.* in 2010. Nevertheless, only one isolated emission band at 1220 nm was observed with a narrow bandwidth of ~60 nm.[9] Despite these inspiring progresses, there remain significant challenges which limit the practical application for BDF/BEDF. One of them is the ambiguity and controversy for the origin of bismuth active center, though numerous physical models, including Bi^{5+}, Bi^{3+}, Bi^{+}, Bi clusters and negative charged Bi_2^{-} dimer, have been proposed to explain the NIR emitting Bi centers. Unfortunately, none of these models show comprehensive evidences.[10–12] Another

[a]Corresponding author: Qiancheng.zhao@unsw.edu.au

significant challenge is the development of broadband application for BEDF, Zinat and J. Zhang did some pioneer work in the spectral characterization of BEDF. However, only the spectral property of BEDF was specified under single 830 nm pumping,[13] in which only one or two dominant luminescence bands were observed. Y. H. Luo firstly made the efforts for 532 and 808 nm dual pumping.[14] Nevertheless, it only investigated the dependence of emission wavelengths for BACs on the pump wavelength, neither the flat luminescence nor the broadband gain in the 1000-1600 nm was reported for the BEDF. So far, there is no proper pumping scheme for achieving broadband, flat luminescence and gain covering the whole Bi and Er active bands, which may limits the potential of BEDF for extensive applications.

Herein, we report the dual pumping (830 and 980 nm) scheme to flatten and broaden the spectral coverage and bandwidth for homemade multicomponent (Si/P/Al/Ge) BEDF. Firstly, the optical absorption of BEDF is measured and the different absorption peaks are identified. Subsequently, we investigate the emission characteristics of BEDF under single and dual pumping by 830 and 980 nm pumps. We further demonstrate the application of dual pumping scheme on the gain performance of BEDF. The experimental results show that the proposed dual pumping scheme can be employed for broadband optical applications.

The BEDF was fabricated by conventional modified chemical vapor deposition (MCVD) method. The Al_2O_3, Er_2O_3 and Bi_2O_3 were incorporated into the silica substrate tube (Heraeus F300) by *in-situ* solution doping technique. The BEDF sample was drawn with the following parameters: core diameter ~3.5 μm, cladding diameter ~94.2 μm, numerical aperture (NA) ~0.238, and cut-off wavelength λ_c ~852 nm. The dopant concentrations across the fiber core were measured by energy disperse X-ray analysis (EDX) (see Figure 1(a) and (b)), the estimated dopant concentrations (the average value of selected points in Figure 1(a)) of BEDF are [Ge] ~1.68, [Bi] ~0.35, [Er] ~0.07, [Al]~ 0.07 atom%, respectively. The content of phosphorous (P) and silica (Si) was also estimated to be ~4.73 and 21.5 at.% through theoretical calculation of the refractive index profile (RIP) of BEDF, the sharp dip in the center of RIP represents the Bi depletion during the preform collapse process under ~1900 °C ($T_{Bi\text{-}boiling}$ ~ 1564°C).

The absorption spectrum from 500 to 1600 nm was measured by cut-back method, Figure 1(c) shows isolated Bi-related absorption bands peaking at 500 (A), 700 (B), 820 (C) and 1400 nm (F). Meanwhile, the absorption spectrum in the 900-1100 nm features several overlapped absorption bands centred at 925 nm (D), 976 nm and 1000 nm (E, shoulder peak), these peaks have been

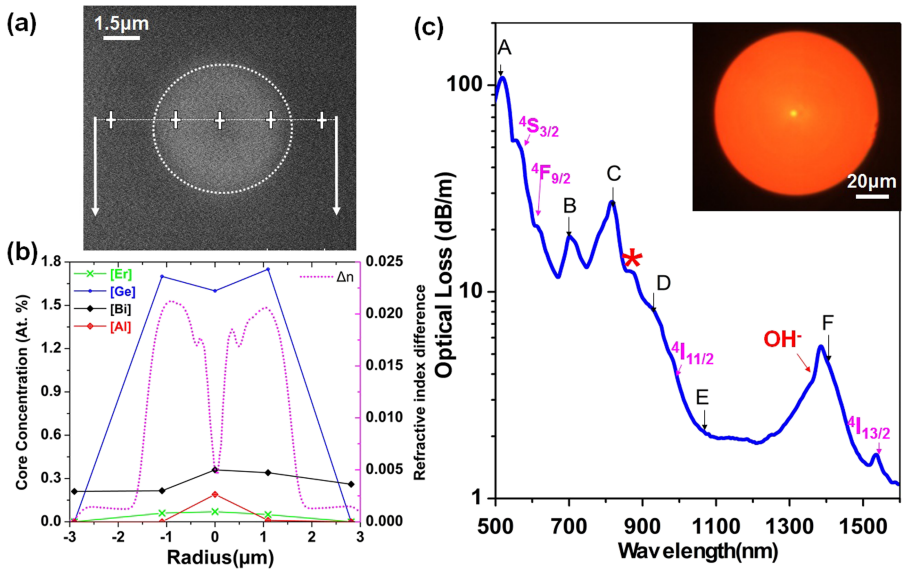

FIG. 1. (a) Scanning electron microscopy (SEM) image in the BEDF core region. (b) Concentration distribution and RIP across the core region indicated by downward arrows shown in (a). (c) Optical absorption spectrum of BEDF in the range 500-1600 nm. The inset shows the microscopic imaging of BEDF cross section.

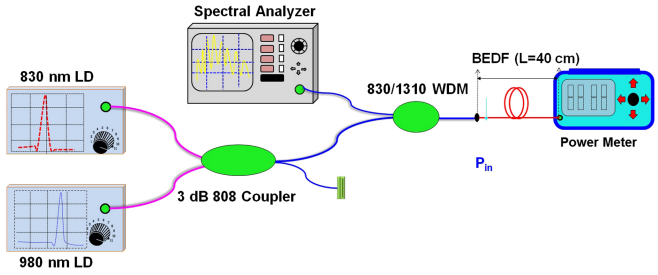

FIG. 2. Dual pumping experimental setup for backward luminescence measurement.

identified to be associated with BAC-Ge,[15,16] Er^{3+},[17,18] and BAC-Al,[19,20] respectively. According to the previous study, multiple BACs can be excited under single 830 nm pumping while 980 nm pump is proved to be quite effective for Er^{3+} with a large absorption cross section $\sim 31.2 \times 10^{-22}$ cm^2 (Si/Al substrate).[13] Hence, 830 and 980 nm pumps are selected here to enhance and tune the bandwidth for our multicomponent BEDF. The luminescence measurement setup is depicted in Figure 2.

The 830 and 980 nm pigtailed laser diodes (LD) were launched into the input end of 3dB 808 coupler and the 810/1310 WDM, the BEDF was spliced with output end of 1310 beam with ~1 dB splice loss. The emission signal was recorded by the backward optical spectral analyzer (OSA) to eliminate the influence of residual pump power. A short length (~40 cm) of BEDF was tested and a digital power meter was placed at the end of BEDF to monitor the unabsorbed pump power.

Firstly, the luminescence spectrum excited by single 8.26 mW 830 nm pumping is shown in Figure 3(a), broadband emission is observed in the range 950-1600 nm with a dominant peak around 1430 nm. After compensating the WDM's insert loss, two more luminescence bands (blue dashed curve) centred at 1100 nm and 1538 nm are clearly seen. Since the emission spectrum features a complicated profile, Gaussian decomposition is applied to identify the complex emission bands. As shown in Figure 3(b), four distinct luminescence bands ascribed to BAC-Al (~1100 nm), BAC-P (~1310 nm), BAC-Si (~1425 nm) and Er^{3+} (~1538 nm) are separated. Meanwhile, the emission spectra versus 980 nm pump power are plotted in Figure 3(d). It is seen that there is no emission for

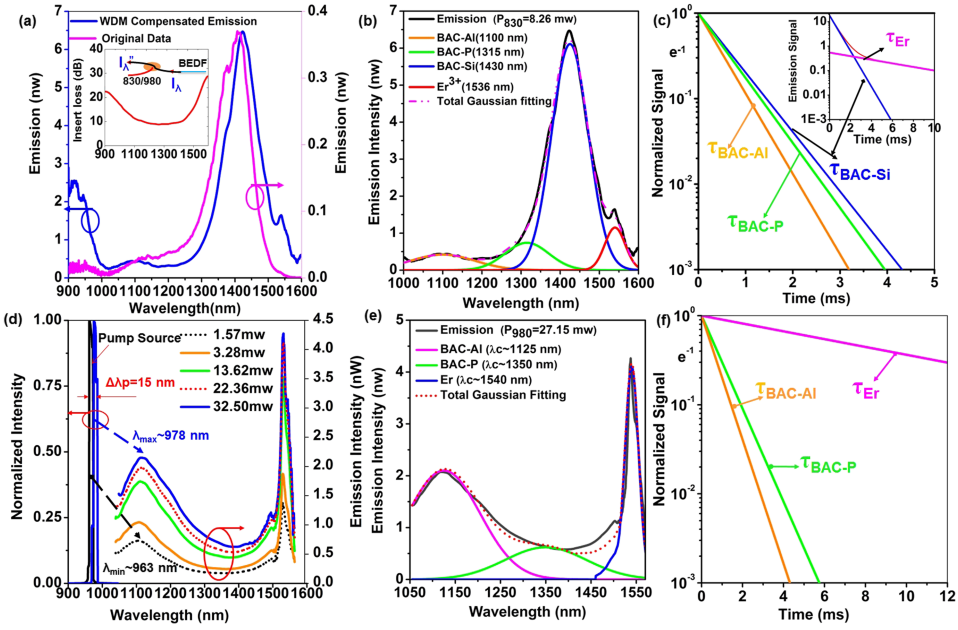

FIG. 3. (a) Luminescence spectrum under single 830 nm pumping at 8.26 mW. The inset shows the WDM's insert loss. (b) Gaussian decomposition for luminescence spectrum in (a). (c) Luminescence decay for BACs and Er^{3+} under 830 nm pumping (d) Luminescence spectra versus 980 nm pump power. (e) Gaussian fitting for luminescence spectrum under single 980 nm pumping at 27.15 mW. (f) Luminescence decay for BACs and Er^{3+} under 980 nm pumping.

BAC-Si while the emission peak at 1120 nm shifts to longer wavelength (Δλ~ 18 nm) with increasing pump wavelength (from 963 to 976 nm). This coincides with the previous study that the BAC-Al emission show large dependence on the pumping wavelength.[21,22] Also, the Gaussian decomposition reveals the presence of BAC-P (λ~1350 nm) band In addition to the dominant emission band at 1120 nm (Figure 3(e)).

Further to the Gaussian fitting analysis, the luminescence decay at different emission wavelengths were measured based on time domain methodology (see Figure 3(c) and (f)). The single exponential decay with different slopes (except the Er^{3+} decay which overlaps with BAC-Si under 830 nm pumping) correspond to different emission lifetimes ascribed to individual BAC identified by the Gaussian fitting. Upon all the emission parameters obtained under 830 and 980 nm pumping, the emission cross sections can be calculated via the Fuchtbauer-Ladenburg relations in equation (1):[23]

$$\sigma_e = \frac{\lambda}{4\pi n^2 \tau \Delta V}\left(\frac{ln2}{\pi}\right)^{1/2} \tag{1}$$

Where λ is the central emission wavelength, ΔV is the FWHM of the emission in Hertz, τ represents the emission lifetime and n is the refractive index of fiber core (n=1.49). The emission cross sections for BACs are hence summarized in Table I.

Seen from Table I, it is obvious that BAC-Al, BAC-P can be excited under both 830 and 980 nm pumping but with noticeable peak wavelength drift ($\Delta\lambda_{BAC\text{-}Al}$ ~25 nm and $\Delta\lambda_{BAC\text{-}P}$ ~40 nm). Furthermore, 980 nm pumping induces larger bandwidth for BAC-Al and BAC-P compared to 830 nm pumping. Under 830 nm pumping, the emission cross section б of BAC-Si was calculated to be 3.7×10^{-20} cm^{-2}, which is 3.6 and 1.5 times bigger than that of BAC-Al and BAC-P. This indicates that BAC-Si benefits most from 830 nm pumping since 830 nm (~12000 cm^{-1}) is directly at excited state BAC-Si2.[15] Although smaller emission cross sections for BAC-Al and BAC-P are obtained under 980 nm pumping, the long lifetime ($\tau_{BAC\text{-}Al}$ ~844 μs and $\tau_{BAC\text{-}P}$ ~624 μs) reveals the better stability at this wavelength. Subsequently, the dependences of BACs' luminescence intensity on the pump power are also plotted in Figure 4(a)–(c). Under 830 nm pumping (Figure 4(a)), the emission intensity of BAC-Si increases rapidly with a slope efficiency of approximate 2.16 nW/mW and approaches saturation at 2.8 mW input power. Nevertheless, the remaining three emission centers, including Er^{3+}, BAC-P and BAC-Al, show linear increase with slope efficiencies of 0.13, 0.11 and 0.057 nW/mW, respectively.

In contrast to 830 nm pumping, the emission intensity for Er^{3+} firstly reaches saturation at 10 mW with a slope efficiency of ~0.42 nW/mW under 980 nm pumping. Noteworthily, the BAC-Al emission band features two distinct slope efficiencies of 0.09 and 0.03 nW/mW before and after the saturation pump power of Er^{3+}. It indicates the energy transfer process from Er^{3+} ($^4I_{11/2}$) to BAC-Al. Figure 4(c) illustrates the conversion efficiencies as a function of 830 and 980 nm input power. It is clearly that the 830 nm pump achieves higher conversion efficiency up to 1×10^{-3} level, which is nearly one order of magnitude bigger than 980 nm pumping. The conversion efficiency ratio of 830 nm to 980 nm remains at ~2.5 due to the existence of dominant BAC-Si band for 830 nm pumping. Considering the different slope efficiencies and pump efficiencies for single pumping of 830 and 980 nm, it enables us to adjust the pump ratio between 830 and 980 nm pumps to flatten and broaden the NIR luminescence for BEDF. Since the pump power ratio between 980 and 830 nm can be adjusted from 0.032 to 116 in our pump systems. Moreover, since the BAC-Al band features the widest bandwidth, it is reasonable to equalize peak intensity for BAC-Al ($Slope_{BAC\text{-}Al}$~ 0.057 and 0.09 nW/mW for 830 and 980 nm, respectively) and BAC-Si ($Slope_{BAC\text{-}Si}$~ 2.16 nW/mW for 830 nm pumping) by tuning the pump ratios. By calculation based on slope efficiencies for BAC-Si and

TABLE I. Emission parameters of luminescence spectra under single 830 and 980 nm pumping.

Pump (nm)	BAC-Al λc (nm)	Δν (nm)	τ (μs)	б (cm^{-2})	BAC-P λc (nm)	Δν (nm)	τ (μs)	б (cm^{-2})	BAC-Si λc (nm)	Δν (nm)	τ (μs)	б (cm^{-2})
830	1100	193.1	460	1.03×10^{-20}	1315	131.9	564	2.5×10^{-20}	1425	110.7	626	$3.7*10^{-20}$
980	1125	202.5	844	0.58×10^{-20}	1350	200.2	624	1.65×10^{-20}	…	…	…	…

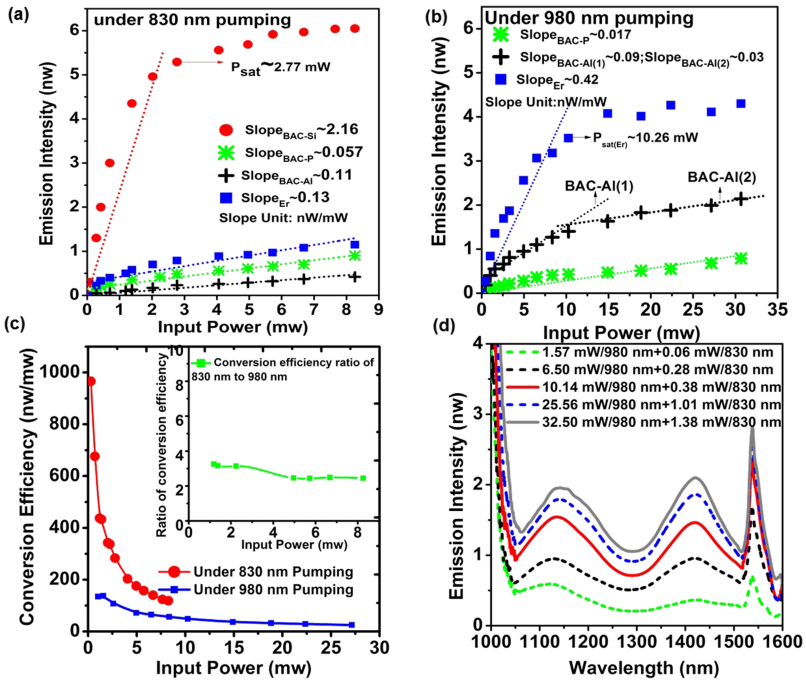

FIG. 4. (a) Dependence of emission intensity of BACs and Er^{3+} under (a) 830 nm pumping. (b) 980 nm pumping. (c) Conversion efficiency (defined as the ratio of integrated emission intensity between 1000 to 1600 nm to the pump power) for single pumping of 830 and 980 nm respectively. The inset shows the conversion efficiency ratio of 830 to 980 nm pumping. (d) Flat, balanced and broad luminescence spectra by tuned power combinations of 830 and 980 nm dual pumping.

BAC-Al, an optimal pump ratio of ~25 (980 VS 830 nm) is obtained to flatten the whole luminescence spectrum in the range 1000-1600 nm, as shown in Figure 4(d). The luminescence spectra are obtained by power ratios ranging from 23.2 to 25.6, which is consistent with the analysis of the emission slope efficiencies.

Further to luminescence characterization, dual pumping scheme is applied on the on-off gain performance of BEDF to exploit the BEDF's potential as the practical gain medium. The experimental configuration is shown in Figure 5(a): The input WLS signal was modulated by a chopper which was synchronised with the lock-in amplifier so that only signal in-phase was collected by lock-in amplifier. The transmitted signal was picked up by the InGaAs photodetector (Δλ~ 900-1700 nm). The same length of ~40 cm of BEDF was selected to keep consistency with the emission test. The on-off gain is defined in equation 2:

$$G_{on-off} = \frac{1}{L} \times 10 \times \log\left(\frac{T_{on}}{T_{off}}\right) \tag{2}$$

Where T_{on} and T_{off} represent the transmission signal with the pump on and off, respectively. L is the length of BEDF.

The on-off gain spectra under single and dual pumping are plotted in Figure 5(b)–(d). For 830 nm pumping (Figure 5(b)), broadband gain is obtained in the range 1300-1600 nm while considerable ESA band is seen from 950 to 1300 nm which is due to ESA of BAC-Al.[20,24] By Gaussian decomposition, separate gain bands peaking at 1400 nm (BAC-Si) and 1536 nm (Er^{3+}) are observed. In contrast, there is no gain for BACs under 980 nm pumping (~32.5 mW) except the Er^{3+} gain band (~0.8 dB/m). The gain dependences of BAC-Si and Er^{3+} son 830 nm pump power are demonstrated in Figure 5(c). It is seen that the gain slopes for BAC-Si and Er^{3+} are 0.2 and 0.06 dBm^{-1}/mW, respectively. Since both 980 nm and 830 nm contribute to the gain of Er^{3+}, in order to balance the gain between BAC-Si and Er^{3+}, as well as to achieve the maximum amplification. The dual pump scheme is set in the following step: keep maximum 980 nm pump power (~32.5 mw) and increase 830 nm pump power gradually to flatten the gain in the range 1300-1600 nm (based on the relation of gain slopes in Figure 5(c)) Figure 5(d) shows the gain spectra obtained by different dual pump combinations. With increasing

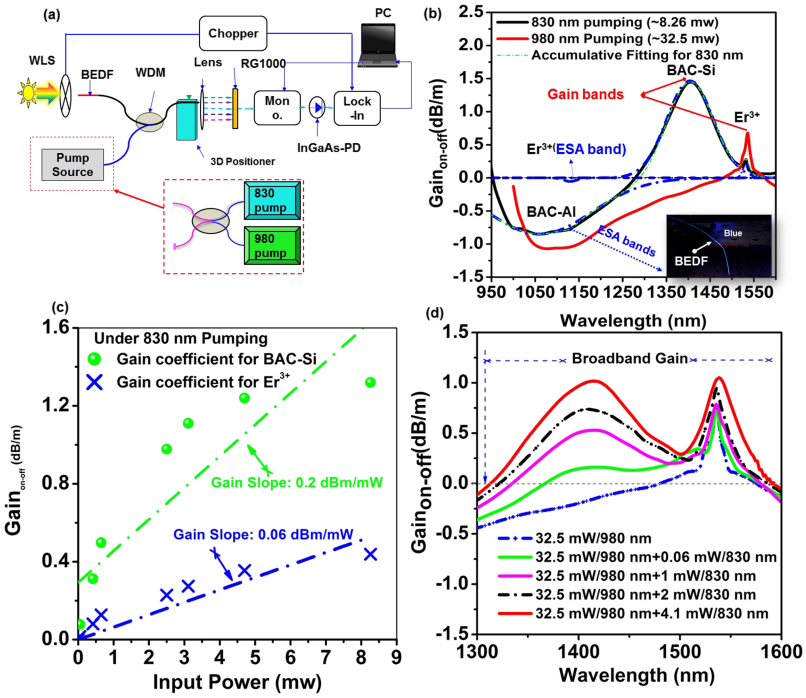

FIG. 5. (a) Experimental setup of on-off gain measurement. (b) On-off gain under single pumping of 8.26 mW 830 nm and 32.5 mW 980 nm. (c) The dependence of Gain on single 830 nm pump power. (d) On-off gain under power combinations of dual pumping.

830 nm pump power, the gain coefficients of both BAC-Si and Er band increase smoothly. Due to the higher conversion efficiency for BAC-Si, the gain of BAC-Si grows faster than that of Er^{3+}. Both gain bands reach the same peak (~1.1 dB/m) when the 830 nm pump power is 1/8 (~4.1 mW) of the 980 nm pump power and the flat, and balanced gain spectrum covers over 300 nm, which is nearly 3 and 5 times broader compared to single pumping of 830 and 980 nm, respectively.

Along with previous research and the spectral properties obtained for our multicomponent BEDF, the energy level diagrams are constructed for 830 and 980 nm pumping, respectively. Upon single 830 nm pumping (Figure 6(a)), BAC-Si undergoes resonant absorption from GS to ES2 and decay rapidly to the ES1 where emission at 1430 nm is seen. Meanwhile, BAC-Al and BAC-P also absorb 830 nm photons but with much smaller absorption cross sections, and finally give emissions at 1100 and 1315 nm. Upon strong excitation of 830 nm, blue up-conversion is seen due to the ESA of BAC-Al and Er^{3+} (green) (ES3 →GS for BAC-Al, $^4S_{3/2} \rightarrow {}^4I_{15/2}$ for Er^{3+}). The overall blue colour manifests the dominance of BAC-Al's ESA over Er^{3+} due to the low erbium concentration in the

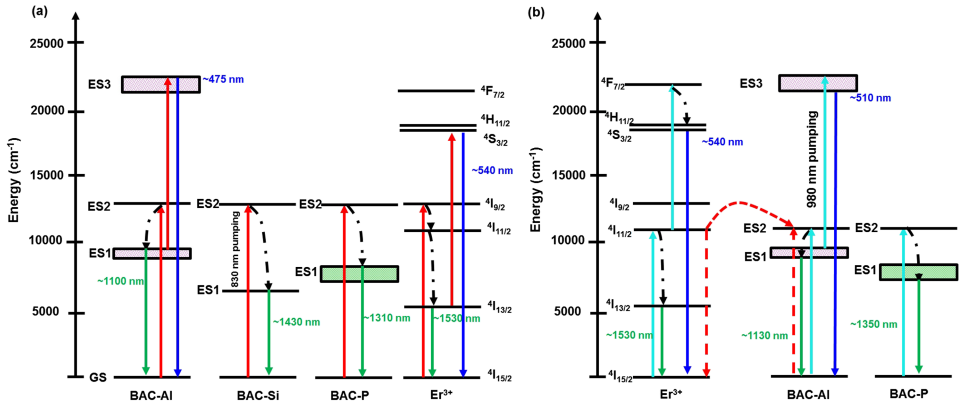

FIG. 6. Energy level diagrams of BEDF based on (a) 830 nm pumping and (b) 980 nm pumping.

BEDF. In the case of 980 nm pumping (Figure 6(b)), the 980 nm photons are initially absorbed by Er^{3+} electrons to $^4I_{11/2}$ manifold from which level parts of electrons directly relax to $^4I_{13/2}$ and give emission at 1530 nm. However, the remaining ions transfer energy from $^4I_{11/2}$ to ES2 of BAC-Al which facilitates the BAC-Al's emission at 1120 nm. This has been evidenced by distinct emission slope efficiencies at saturation point of Er^{3+} and longer lifetime (compared with 830 nm pumping) at ES1 of BAC-Al. The blue up-conversion will be seen when strong 980 nm pumping is fulfilled due to BAC-Al transitions. For 830 and 980 nm dual pumping, higher pump efficiency for Er^{3+} and BAC-Al bands are obtained, thus broadband, flat emission and gain spectrum can be achieved by tuning the pump power ratio.

In conclusion, we have performed dual 830 and 980 nm pumping scheme to flatten and broaden the spectral performance for multi-component BEDF. The distinct BACs' spectral characteristics have been identified, including the luminescence lifetime, emission slope efficiency and the emission cross sections. Through the comparison and calculation of different emission slope efficiencies, an optimal power ratio of ~25 (980 VS 830 nm) have been achieved to obtain flat and broad luminescence in the range 1000-1600 nm. Furthermore, the dual pumping scheme is applied to achieve broadband, flat gain covering over 300 nm (1300 -1600 nm), which is 1.5 and 3 times broadened than single pumping of 830 and 980 nm, respectively. These results prove that the presented dual pumping scheme (830 and 980 nm), combined with suitable active component ratios for BEDF, are quite promising for a wide range of broadband optical applications such as uniform NIR ASE source, broadband fiber amplifier, and fiber laser.

ACKNOWLEDGMENTS

This work was supported by NSFC (61520106014, 61405014 and 61377096), STCSM (SKLSFO2015-01 and 15220721500), Open Fund of SKLFPM (DHU) (LK1502), and Fund of IPOC (BUPT) (IPOC2016ZT07).

[1] K. Murata, Y. Fujimoto, T. Kanabe, H. Fujita, and M. Nakatsuka, "Bi-doped SiO_2 as a new laser material for an intense laser," Fusion Engineering and Design **44**, 437–439 (1999).
[2] E. M. Dianov, A. V. Shubin, M. A. Melkumov, O. I. Medvedkov, and I. A. Bufetov, "High-power cw bismuth-fiber lasers," Journal of the Optical Society of America B **24**, 1749–1755 (2007).
[3] I. Razdobreev, L. Bigot, V. Pureur, A. Favre, G. Bouwmans, and M. Douay, "Efficient all-fiber bismuth-doped laser," Applied Physics Letters **90**, 031103 (2007).
[4] I. A. Bufetov, M. A. Melkumov, S. V. Firstov, K. E. Riumkin, A. V. Shubin, V. F. Khopin, A. N. Guryanov, and E. M. Dianov, "Bi-doped optical fibers and fiber lasers," IEEE Journal of Selected Topics in Quantum Electronics **20**, 111–125 (2014).
[5] V. V. Dvoyrin, A. V. Kir'yanov, V. M. Mashinsky, O. I. Medvedkov, A. A. Umnikov, A. N. Guryanov, and E. M. Dianov, "Absorption, gain, and laser action in bismuth-doped aluminosilicate optical fibers," IEEE J. Quantum Electron. **46**, 182–190 (2010).
[6] B. Ainslie, S. Craig-Ryan, S. Davey, J. Armitage, C. Atkins, J. Massicott, and R. Wyatt, "Erbium doped fibres for efficient optical amplifiers," IEE Proceedings-J: Optoelectronics, 205–208 (1990).
[7] W. J. Miniscalco, "Erbium-doped glasses for fiber amplifiers at 1500 nm," Journal of Lightwave Technology **9**, 234–250 (1991).
[8] M. Peng, N. Zhang, L. Wondraczek, J. Qiu, Z. Yang, and Q. Zhang, "Ultrabroad NIR luminescence and energy transfer in Bi and Er/Bi co-doped germanate glasses," Opt. Express **19**, 20799–20807 (2011).
[9] Y. Q. Qiu, X. Y. Dong, and C. L. Zhao, "Spectral characteristics of the erbium-bismuth co-doped silica fibers and its application in single frequency fiber laser," Laser Physics **20**, 1418–1424 (2010).
[10] M. Peng, G. Dong, L. Wondraczek, L. Zhang, N. Zhang, and J. Qiu, "Discussion on the origin of NIR emission from Bi-doped materials," Journal of Non-Crystalline Solids **357**, 2241–2245 (2011).
[11] J. Zheng, L. Tan, L. Wang, M. Peng, and S. Xu, "Superbroad visible to NIR photoluminescence from Bi^+ evidenced in $Ba_2B_5O_9Cl$: Bi crystal," Optics Express **24**, 2830–2835 (2016).
[12] V. O. Sokolov, V. G. Plotnichenko, and E. M. Dianov, "Origin of broadband near-infrared luminescence in bismuth-doped glasses," Optics Letters **33**, 1488–1490 (2008).
[13] Z. M. Sathi, J. Zhang, Y. Luo, J. Canning, and G. D. Peng, "Spectral properties and role of aluminium-related bismuth active centre (BAC-Al) in bismuth and erbium co-doped fibres," Optical Materials Express **5**, 1195 (2015).
[14] Y. Luo, J. Wen, J. Zhang, J. Canning, and G. D. Peng, "Bismuth and erbium codoped optical fiber with ultrabroadband luminescence across O-, E-, S-, C-, and L-bands," Opt. Lett. **37**, 3447–3449 (2012).
[15] S. Firstov, V. Khopin, I. Bufetov, E. Firstova, A. Guryanov, and E. Dianov, "Combined excitation-emission spectroscopy of bismuth active centers in optical fibers," Optics Express **19**, 19551–19561 (2011).
[16] S. Firstov, S. Alyshev, M. Melkumov, K. Riumkin, A. Shubin, and E. Dianov, "Bismuth-doped optical fibers and fiber lasers for a spectral region of 1600-1800 nm," Optics Letters **39**, 6927–6930 (2014).
[17] Y. Chen, Y. Huang, M. Huang, R. Chen, and Z. Luo, "Spectroscopic properties of Er^{3+} ions in bismuth borate glasses," Optical Materials **25**, 271–278 (2004).

[18] T. Wei, Y. Tian, C. Tian, X. Jing, J. Zhang, L. Zhang, and S. Xu, "Optical spectroscopy and population behavior between $^4I_{11/2}$ and $^4I_{13/2}$ levels of erbium doped germanate glass," Optical Materials Express **4**, 2150 (2014).
[19] E. M. Dianov, "Bismuth-doped optical fibres: A new breakthrough in near-IR lasing media," Quantum Electronics **42**, 754–761 (2012).
[20] K. E. Riumkin, M. A. Melkumov, I. A. Varfolomeev, A. V. Shubin, I. A. Bufetov, S. V. Firstov, V. F. Khopin, A. A. Umnikov, A. N. Guryanov, and E. M. Dianov, "Excited-state absorption in various bismuth-doped fibers," Optics Letters **39**, 2503–2506 (2014).
[21] M. P. Kalita, S. Yoo, and J. Sahu, "Bismuth doped fiber laser and study of unsaturable loss and pump induced absorption in laser performance," Optics Express **16**, 21032 (2008).
[22] M. P. Kalita, S. Yoo, and J. K. Sahu, "Influence of cooling on a bismuth-doped fiber laser and amplifier performance," Appl. Opt. **48**, G83–G87 (2009).
[23] X. Meng, J. Qiu, M. Peng, D. Chen, Q. Zhao, X. Jiang, and C. Zhu, "Near infrared broadband emission of bismuth-doped aluminophosphate glass," Optics Express **13**, 1628 (2005).
[24] Z. Qiancheng, Y. Luo, and G.-D. Peng, "Investigation of unsaturable absorption and excited state absorption on Bi/Er co-doped fibers," in *Bragg Gratings, Photosensitivity, and Poling in Glass Waveguides*, 2016, p. JM6A.7.